CORROSION PRODUCTS PHASE IDENTIFICATION USING MICRO-RAMAN AND FTIR

Dušan MAJTÁS [1,2], Petra MÁCOVÁ [1]

[1]*Institute of Theoretical and Applied Mechanics, Prague, Czech Republic, EU*
majtas@itam.cas.cz,
[2]*Faculty of Sciences, Department of Chemistry, Masaryk University, Brno, Czech Republic, EU*

Abstract

Phase identification of corroded metal objects might be problematic because corrosion products are usually a complex mixture of different phases. Furthermore, some of present phases may be either semi-crystalline or amorphous. The most suitable procedure is to use X-ray diffraction (XRD), for identification of crystalline phases in bulk, in combination with micro-Raman spectroscopy to obtain information on smaller scale and given location. Micro-Raman spectroscopy identifies crystalline and semi-crystalline phases. The literature also reports of the application of Mössbauer spectroscopy to identify amorphous phases. In this work, the combined use of Fourier-transform infrared spectroscopy (FTIR) and Raman spectroscopy is evaluated. The methods may be interchangeable to some point. But is it safe to assume that all phases present can be detected?

Keywords: Corrosion, micro-Raman spectroscopy, FTIR

1. INTRODUCTION

Corrosion products of iron are a complex mixture of crystalline, semi-crystalline and sometimes amorphous oxides and oxy-hydroxides. Information about their identification and spatial distribution within the corroded body is of interest for the comprehension of the corrosion processes, for corrosion protection and in preservation of cultural heritage [1-6]. The strong overlap of the signals from the components in such complex samples, forces the scientist to resort to a combination of analytical techniques. One common approach used to identify the phases present in iron corrosion products, is to combine XRD, Raman spectroscopy and Mössbauer spectroscopy [5-7]. The combination of XRD with FTIR and Mössbauer spectroscopy has been also reported [8,9]. Sometimes Energy-dispersive X-ray spectroscopy (EDS) is used alone without additional phase analysis [1-3] or in combination with XRD and Raman. Scanning electron microscopy (SEM) is useful to optically verify the crystalline structure of corrosion products [4,10]. Given that Mössbauer spectroscopy might not be available, could another combination of analytical techniques provide suitable results for phase identification? Samples used in this paper are from the specimen obtained from main railway station in Prague used in a previous work [11]. XRD characterization of corrosion products was already done previously [11,12] therefore has not been replicated here.

2. METHODOLOGY

For the phase analysis of the corrosion product layers, both micro-Raman and FTIR were used on the samples prepared for microscopic observations as shown in previous work [11]. Samples were obtained from the same specimen embedded into Araldite resin. Cross-sections of these samples have been prepared by grinding and polishing. Linear and area mapping have been performed at selected locations on the sample. Mapping was used to verify the layered structure observed under optical microscope.

Raman spectra were collected on the DXR Raman microscope (Thermo Scientific). Experimental setup was as follows: spectral range 1800-50 cm^{-1}; mapping step 1 and 10 μm; grating 1800 lines per mm; spectral resolution 2 cm^{-1}; focusing 20×; 0.1 mW laser power at 532 nm wavelength.

ATR FTIR spectra were collected using infrared microscope Nicolet iN10 (Thermo Scientific) equipped with a liquid nitrogen cooled MCT detector, KBr beamsplitter and germanium micro attenuation total reflectance (ATR) crystal. Experimental setup was as follows: line mapping step 20 and 50 μm; rectangular aperture 20×100 μm; 128 scans per spectrum; spectral range 4000 - 675 cm^{-1} using the spectral resolution 8 cm^{-1}.

3. PHASE IDENTIFICATION - DISCUSSION

Data have been collected using ATR-FTIR and micro-Raman spectroscopy perpendicular to the corrosion product layers. Spectra obtained by both methods showed that the layered structure observed under optical microscope reflects differences in the layer composition. Thickness of maghemite layers observed under optical microscope is in most situations 5-10 μm. Unlike micro-Raman, in case of the ATR-FTIR technique, because of the low spatial resolution compared to the layer thickness, maghemite spectra have not been measured as a single phase spectra but as a combination of bands corresponding to two phases, maghemite and goethite.

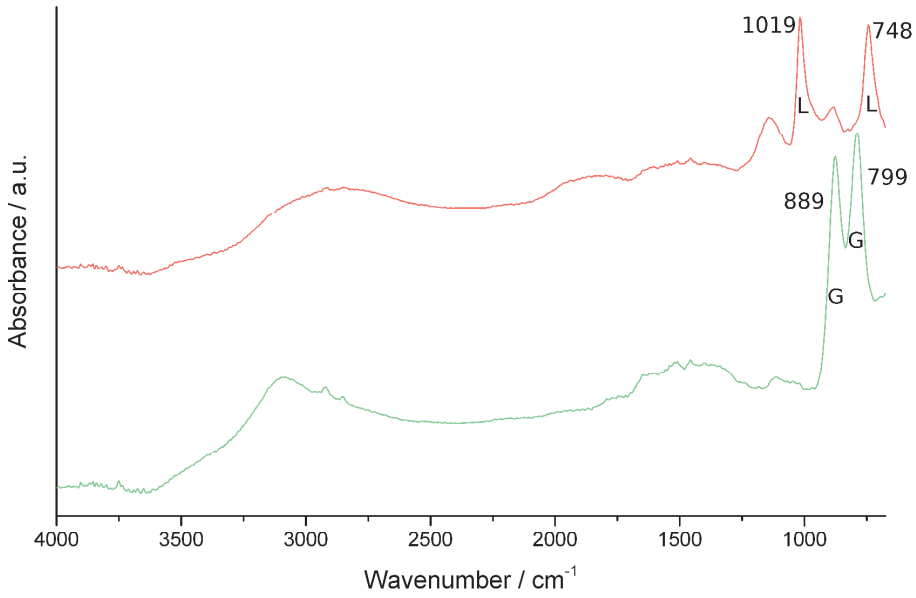

Figure 1 Example of FTIR spectra obtained from different layers. Significant peaks of lepidocrocite - L, significant peaks of goethite -G

Lepidocrocite (γFeOOH) and goethite (αFeOOH) could be easily distinguished in the FTIR spectra by their characteristic absorption bands. Namely, at 799 (795) cm^{-1} and 889 (883) cm^{-1}, for goethite, and at 748 (750) cm^{-1} and 1019 (1020) cm^{-1} for lepidocrocite. They are in excellent agreement with literature values, reported in parenthesis [13]. Two examples of collected spectra are illustrated in **Figure 1**. Some of the spectra showed magnetite (Fe_3O_4) - characteristic absorption band at 590 (588) cm^{-1} [8], but also contained goethite.

According to literature [8,13] absorption bands of iron oxides are near the edge between mid-IR and far-IR or directly in far-IR [14,15] region. The case of magnetite and maghemite (γFe_2O_3) is of relevance here. Iron oxides in mid-IR have bands in same position and show strong overlap, thus, ATR-FTIR in mid-IR alone may not be sufficient for phase identification of corrosion products. Additional analysis of sample in form of tablet with KBr was used in exchange of mapping capability wavenumber range was increased (4000-450 cm^{-1}). Powdered sample 1 was measured in transmission mode in form of KBR pellets. The spectrum obtained showed bands at 625 and 590 cm^{-1}. Low intensity band around 565 cm^{-1}, could be identified. There might be other bands present there, but could not be clearly identified do to sloped baseline. According to [16],

maghemite bands are at 630, 590, 570, 450 and 400 cm^{-1}, magnetite bands at 590 and 400 cm^{-1}, hematite (αFe_2O_3) bands at 540, 470 and 400 cm^{-1}.

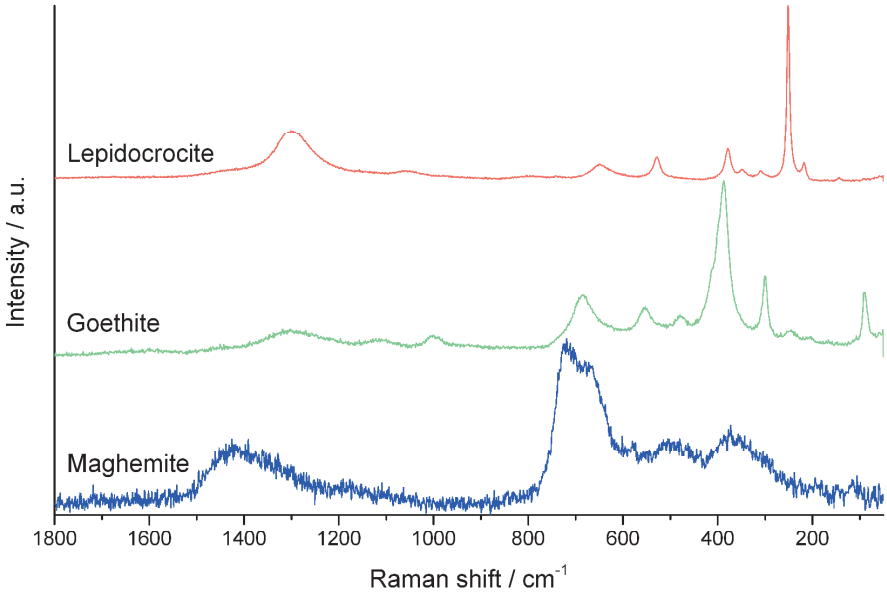

Figure 2 Raman spectra of identified phases

Micro-Raman spectra of pure phases could be obtained, taking advantage of the possibility of focusing the laser beam on a small area (c.ca 1 micron) as shown on the **Figure 2**. Lepidocrocite, goethite and maghemite, the first two detected also by ATR-FTIR, have been identified in Raman mapping. Lepidocrocite is present either on the surface of the corrosion product or on the surface of cracks in the corrosion products, where the crack is connected to the outer surface. Inside the corrosion product, the layered structure containing goethite and maghemite, each in separate layers, can be optically distinguished, as observed in the obtained maps on the **Figure 3**.

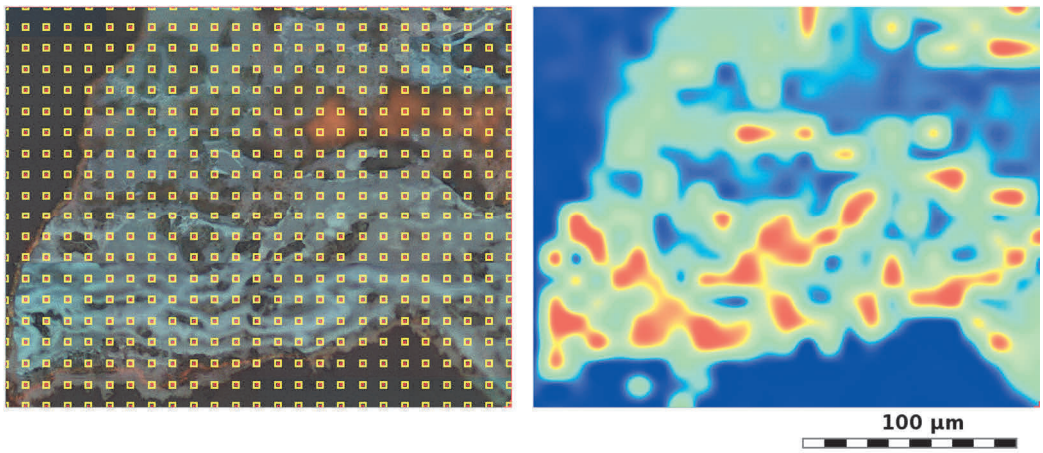

Figure 3 Area of sample showing the corner of the sample. On the left side as seen with the microscope of the micro-Raman instrument (overlay showing the 2D scanning matrix on scale). On the right side intensity contour map of maghemite is shown. Intensity is decreasing from red to blue.

As noted above, the thickness of maghemite layers was below the ATR-FTIR spatial resolution employed, resulting in mixed goethite-maghemite spectra.

Literature sources [17] also suggest the possibility that the Raman spectra previously identified as maghemite might be in fact superposition of maghemite and magnetite. This may be clear by observing the spectrum of maghemite in **Figure 2**, since, magnetite has significant peak at 672 cm^{-1} and additional two low intensity peaks at 535 cm^{-1} and 300 cm^{-1}. It is worth mentioning that formation of maghemite by conversion of magnetite under effect of laser used in Raman spectroscopy, has been also reported [11].

Summarizing findings of both methods: lepidocrocite and goethite have been detected by both methods with no doubt. Additional phase which is not iron oxy-hydroxide is present. By using only ATR-FTIR Nicolet iN10 “some iron oxide” may be identified. By combining FTIR and Raman analysis bands of iron oxide present in the corrosion products could be identified as maghemite.

ATR-FTIR with mapping capability could be used to identify lepidocrocite and goethite. For proper phase analysis of iron oxides far-IR range was needed. In case far-IR is not accessible, the XRD should be used for this purpose.

In conclusion, to take advantage of the combined use of the two techniques, one can do a fast mapping of the surface of interest with FTIR and focus on the details of interest with micro-Raman, which is more suitable as a local technique.

For identification of iron oxides, extension of the range to the far-IR region, is recommended.

4. CONCLUSIONS

Presence of lepidocrocite and goethite in the specimen has been confirmed by both methods. Maghemite was identified when ATR-FTIR method with broader wavenumber range capable to analyze far-IR was used.

Compared to micro-Raman, ATR-FTIR mapping can be done significantly faster, unless imaging detector is used. The map would not be so detailed compared to micro-Raman, due to the larger aperture used. To obtain the best from both techniques, preliminary, albeit low resolution, 2D map of large areas of the sample, can be collected, and particular interesting zones could be selected to be further observed by area 2D area mapping using micro-Raman. As used in previous works [11,12].

Base starting point is to have the phase identification of the bulk sample, for which XRD is suitable method. FTIR itself could not replace Mössbauer spectroscopy, which is, on the other hand, not as common as FTIR, but in the combination of several other analytical methods such as XRD and micro-Raman it can be used to phase identification of the sample.

ACKNOWLEDGEMENTS

This article was prepared and carried out in the scope of LO 1219 project under the Ministry of Education, Youth and Sports National sustainability programme I of Czech Republic.

REFERENCES

[1] FUENTE, D., ALCÁNTARA, J., CHICO, B., DÍAZ, I., JIMÉNEZ, J. A., MORCILLO, M. Characterisation of rust surfaces formed on mild steel exposed to marine atmospheres using XRD and SEM/Micro-Raman techniques. *Corrosion Science,* 2016, vol. 110, pp. 253-264.

[2] NEFF, D., DILLMANN, P., BELLOT-GURLET, L., BERANGER, G. Corrosion of iron archaeological artefacts in soil: characterization of the corrosion system. *Corrosion Science,* 2004, vol. 47, pp. 515-535.

[3] VEGA, E., DILLMANN P., FLUZIN, P. A study on species transport in the corrosion products of ferrous archaeological analogues - a contribution to the modelling of iron long term corrosion behavior. In *EUROCORR 2004: International Conference.* Frankfurt am Main: DECHEMA e.V., [CD-ROM] 2004, art. no. 218, pp. 1-10.

[4] DHAIVEEGAN, P., ELANGOVAN, N., NISHIMURA, T., RAJENDRAN, N., Electrochemical Characterization of Carbon and Weathering Steels Corrosion Products to Determine the Protective Ability Using Carbon Paste Electrode (CPE). *Electroanalysis*. 2014. vol. 26, pp. 2419-2428.

[5] DIAZ, I., CANO, H., FUENTE, D., CHICO, B., VEGA, J. M., MORCILLO, M., Atmospheric corrosion of Ni-advanced weathering steels in marine atmospheres of moderate salinity. *Corrosion Science,* 2013, vol. 76, pp. 348-360.

[6] YAMASHITA, Masato, MISAWA, Toshishei, OH, S. J., BALASUBRAMANIAN, R., COOK, D. C. Mössbauer spectroscopic study of X-Ray amorphous substance in the rust layer of weathering steel subjected to long-term exposure in North America. *Corrosion Engineering,* 2009, vol. 49, pp. 133-144.

[7] ANTUNES, R. A., ICHIKAWA, R.U., MARTINEZ, L.G., COSTA, I. Characterization of Corrosion Products on Carbon Steel Exposed to Natural Weathering and to Accelerated Corrosion Tests. *International Journal of Corrosion,* 2014, vol. 109, pp. 1-9.

[8] GOTIĆ, M., MUSIĆ, S. Mössbauer, FT-IR and FE SEM investigation of iron oxides precipitated from $FeSO_4$ solutions. *Journal of Molecular Structure,* 2007, vol. 835, pp. 445-453.

[9] BELTRÁN, J. J., NOVEGIL, F. J., GARCÍA, K. E., BARRERO, C. A., On the reaction of iron oxides and oxyhydroxides with tannic and phosphoric acid and their mixtures. *Hyperfine Interactions,* 2010, vol. 195, pp. 133-140.

[10] AMANI-GHADIM, A.R., ALIZADEH, S., KHODAM, F., REZVANI, Z. Synthesis of rod-like -FeOOH nanoparticles and its photocatalytic activity in degradation of an azo dye: Empirical kinetic model development. *Journal of Molecular Catalysis A: Chemical.* 2015, 2015, vol. 408, pp. 60-68.

[11] MAJTÁS, D., PERÉZ-ESTÉBANEZ, M., KREISLOVÁ, K., MÁCOVÁ, P. Srovnání koroze historických a moderních materiálů na bázi železa. *Fórum pro konzervátory-restaurátory,* 2016, vol. 2016, pp. 74-79.

[12] MAJTÁS, D., MÁCOVÁ, P., KREISLOVÁ, K. Cross-section analysis and mapping using raman spectroscopy. In *METAL 2016: 25th Anniversary International Conference on Metallurgy and Materials*. Ostrava: TANGER, 2016, pp. 531-536.

[13] LEFU, M., LIBING, L., ZISE, W., CHUNCHUN, X. Interactions between Phosphoric/Tannic Acid and Different Forms of FeOOH. *Advances in Materials Science and Engineering,* 2015, vol. 199, pp 1-10.

[14] GLOTCH, T. D., ROSSMAN, G. R. Mid-infrared reflectance spectra and optical constants of six iron oxide/oxyhydroxide phases. *Icarus,* 2009. no. 204 pp. 663-671.

[15] CHERNYSHOVA, I. V., HOCHELLA, M. F., MADDEN, A. S. Size-dependent structural transformations of hematite nanoparticles. 1. Phase transition. *Physical Chemistry Chemical Physics,* 2007. vol. 9, no. 14, pp. 1736-1750.

[16] SCHWERTMANN, U., CORNELL, R. M. Methods of Characterization. In: SCHWERTMANN, U. and CORNELL, R. M. *The Iron Oxides in the Laboratory, Preparation and Characterization. 2nd ed.* Weinheim: Wiley-VCH, 2000, Chapter 3, pp. 27-53.

[17] MOLCHAN, I. S., THOMPSON, G. E., LINDSAY, R., SKELDON, P., LIKODIMOS, V., ROMANOS, G. E., FALARAS, P., ADAMOVA, G., ILIEVC, B., SCHUBERT, T. J. S. Corrosion behaviour of mild steel in 1-alkyl-3-methylimidazolium tricyanomethanide ionic liquids for CO_2 capture applications. *RSC Advance,* 2014, vol. 4, pp. 5300-5311.